

# Abnormal metabolic brain network associated with Parkinson's disease: replication on a new European sample

Petra Tomše<sup>1</sup> · Luka Jensterle<sup>1</sup> · Marko Grmek<sup>1</sup> · Katja Zaletel<sup>1</sup> · Zvezdan Pirtošek<sup>2</sup> · Vijay Dhawan<sup>3</sup> · Shichun Peng<sup>3</sup> · David Eidelberg<sup>3</sup> · Yilong Ma<sup>3</sup> · Maja Trošt<sup>2</sup>

Received: 14 December 2016 / Accepted: 14 March 2017 / Published online: 6 April 2017  
© Springer-Verlag Berlin Heidelberg 2017

## Abstract

**Purpose** The purpose of this study was to identify the specific metabolic brain pattern characteristic for Parkinson's disease (PD): Parkinson's disease-related pattern (PDRP), using network analysis of [18F]-fluorodeoxyglucose positron emission tomography (FDG-PET) brain images in a cohort of Slovenian PD patients.

**Methods** Twenty PD patients (age  $70.1 \pm 7.8$  years, Movement Disorder Society Unified Parkinson's Disease Motor Rating Scale (MDS-UPDRS-III)  $38.3 \pm 12.2$ ; disease duration  $4.3 \pm 4.1$  years) and 20 age-matched normal controls (NCs) underwent FDG-PET brain imaging. An automatic voxel-based scaled subprofile model/principal component analysis (SSM/PCA) was applied to these scans for PDRP-Slovenia identification.

**Results** The pattern was characterized by relative hypermetabolism in pallidum, putamen, thalamus, brain stem, and cerebellum associated with hypometabolism in sensorimotor cortex, posterior parietal, occipital, and frontal cortices. The expression of PDRP-Slovenia discriminated PD patients from NCs ( $p < 0.0001$ ) and correlated positively with patients' clinical score (MDS-UPDRS-III,  $p = 0.03$ ). Additionally, its

topography agrees well with the original PDRP ( $p < 0.001$ ) identified in American cohort of PD patients. We validated the PDRP-Slovenia expression on additional FDG-PET scans of 20 PD patients, 20 NCs, and 25 patients with atypical parkinsonism (AP). We confirmed that the expression of PDRP-Slovenia manifests good diagnostic accuracy with specificity and sensitivity of 85–90% at optimal pattern expression cutoff for discrimination of PD patients and NCs and is not expressed in AP.

**Conclusion** PDRP-Slovenia proves to be a robust and reproducible functional imaging biomarker independent of patient population. It accurately differentiates PD patients from NCs and AP and correlates well with the clinical measure of PD progression.

**Keywords** Parkinson's disease · Atypical parkinsonism · FDG-PET · Specific metabolic brain network · Principal component analysis

## Introduction

Parkinson's disease (PD) is the second most common neurodegenerative disorder after Alzheimer's disease, characterized clinically by motor and non-motor clinical features. Other parkinsonian conditions, such as multiple system atrophy (MSA), progressive supranuclear palsy (PSP), or corticobasal degeneration (CBD), have substantially different prognostic outcomes and treatment options, but may present with similar clinical features as PD especially in early disease stages. Differential diagnosis of parkinsonism is often challenging if based on clinical criteria alone. According to postmortem studies, up to one quarter of patients diagnosed clinically as PD proved to have other pathologies at autopsy [1, 2], most frequently MSA or PSP. Thus, it is critical to identify and

**Electronic supplementary material** The online version of this article (doi:10.1007/s00234-017-1821-3) contains supplementary material, which is available to authorized users.

✉ Maja Trošt  
maja.trost@kclj.si

<sup>1</sup> Department of Nuclear Medicine, University Medical Centre Ljubljana, Ljubljana, Slovenia

<sup>2</sup> Department of Neurology, University Medical Centre Ljubljana, Zaloška cesta 2, 1000 Ljubljana, Slovenia

<sup>3</sup> Center for Neurosciences, The Feinstein Institute for Medical Research, Manhasset, NY, USA

validate potential neuroimaging biomarkers to aid precise early clinical diagnosis of PD.

Functional brain imaging with 18F-fluorodeoxyglucose positron emission tomography (FDG-PET) and univariate brain mapping analysis measures regional differences in cerebral glucose metabolism and this technique has been used as a supplementary tool for diagnosis of parkinsonism [3–6] and for monitoring of disease progression [7]. Nevertheless, despite its wide availability, routine use of FDG-PET imaging has not yet been recommended in the current guidelines for the PD clinical practice [8, 9].

Disease-specific metabolic brain networks have been identified for PD, MSA, and PSP using a multivariate spatial covariance technique known as scaled subprofile model (SSM) based on principal component analysis (PCA) on FDG-PET images [10–14]. Additionally, Topographic Profile Rating (TPR), which gives rise to a similarity measure, has been applied prospectively in individual images to quantify pattern expression by a subject score [15]. This analysis evaluates FDG-PET brain images as an objective tool in assessing cerebral metabolic abnormalities and facilitates accurate early differential diagnosis of clinically uncertain parkinsonism [16, 17]. Disease-specific patterns thus play an important role in strengthening the use of FDG-PET imaging in clinical practice of neurodegenerative diseases.

PD-related pattern (PDRP) was initially identified with FDG-PET in a group of PD patients studied in USA as reported previously [11], and has been later replicated in additional independent patient populations in USA, China, and the Netherlands [18–20]. Subject score of PDRP expression was found to be highly reproducible in individual subjects and its ability to accurately discriminate PD patients from healthy controls and atypical parkinsonism has been confirmed. Individual subject scores were also shown to correlate with clinical measures of disease severity [18, 19] and PET indices of presynaptic dopaminergic functioning [7, 21] and to be sensitive to the rates of disease progression and responses to therapies [7, 22].

In this study, we sought (i) to identify PDRP-Slovenia in a population of Slovenian PD patients scanned in University Medical Centre Ljubljana on Siemens Biograph mCT PET/CT scanner; (ii) to validate PDRP-Slovenia by its ability to differentiate PD patients from healthy controls and from patients with atypical parkinsonism; and (iii) to correlate PDRP-Slovenia expression with clinical measures of disease severity. Additionally, our aim was to evaluate its topography and subject expression in comparison to PDRP originally derived in USA, with the primary goal to further validate robustness of PDRP as a reliable disease-related biomarker independent of patient population and PET scanners.

## Materials and methods

### Subjects

Twenty patients with Parkinson's disease (PD) recruited from the Department of Neurology at the University Medical Centre Ljubljana and 20 age-matched ( $p = 0.18$ ) normal controls (NCs) comprised cohort A (Table 1). PD patients were cognitively normal or had mild cognitive impairment (MMSE average  $26.5 \pm 2.8$ , range 21–30). All subjects were scanned with FDG-PET and used for the identification of PDRP-Slovenia metabolic pattern. Diagnosis of PD was made by a movement disorders specialist based on the UK brain bank criteria [22]. PD patients were assessed by Movement Disorder Society Unified Parkinson's Disease Motor Rating Scale (MDS-UPDRS-III) in off stage, approximately 2 h before the PET scan. They were off levodopa for at least 12 h and off dopamine agonist and MAO-B inhibitor for at least 48 h prior scanning.

For prospective validation of the expression of PDRP-Slovenia network, cohort B was recruited with 20 PD patients and 20 NC subjects (Table 1). There was no overlap in subjects between cohort A and cohort B. These additional PD patients were consecutively recruited from the Department of Neurology at the University Medical Centre Ljubljana and were diagnosed by a movement disorders specialist based on the UK brain bank criteria [23] but were not scored by UPDRS scale and were scanned in on stage. The patients from both cohorts had similar disease duration:  $4.3 \pm 4.1$  years in cohort A and  $4.5 \pm 3.7$  years in cohort B. All control subjects in cohorts A and B were healthy volunteers recruited from the local community with no specific inclusion/exclusion criteria.

To demonstrate the specificity of PDRP, we additionally included a group of patients with atypical parkinsonism (cohort C) studied at the Department of Neurology at the University Medical Centre Ljubljana, composed of 14 MSA patients and 11 PSP patients (Table 1) with clinical follow-up diagnosis  $1.6 \pm 0.9$  and  $1.7 \pm 0.6$  years after FDG-PET scan. The study has been approved by the Slovenian Medical Ethics Committee.

To compare PDRP-Slovenia with PDRP originally identified in USA, we also studied cohort D (Table 1) which comprised of 33 non-demented PD patients (male/female 22/11; age  $57 \pm 8$  years; UPDRS motor rating  $32 \pm 16$ ) and 33 healthy controls (male/female 10/23; age  $55 \pm 13$  years) with FDG/PET images from the Feinstein Institute for Medical Research in Manhasset, New York [11]. The patients in this cohort were scanned with FDG-PET after 12 h off medication. Informed consent was obtained from all individual participants included in this study.

**Table 1** Demographic and clinical characteristics

	Slovenia						USA	
	Cohort A		Cohort B		Cohort C		Cohort D	
	PD	NC	PD	NC	MSA	PSP	PD	NC
<i>N</i>	20	20	20	20	14	11	33	33
Age [years] <sup>a</sup>	70.1 ± 7.8	67.2 ± 5.7	71.8 ± 7.3	63.4 ± 10.6	62.0 ± 8.3	72.5 ± 6.8	57.2 ± 8.2	55.0 ± 13.4
Gender [M/F]	16/4	8/12	11/9	8/12	5/9	5/6	22/11	10/23
Hoehn and Yahr	2 (2–4)	–	–	–	–	–	2.5 (1–5)	–
UPDRS-III*	30.4 ± 10.5	–	–	–	–	–	32.0 ± 16.1	–
Disease duration [years]*	–	–	–	–	4.5 ± 3.5	3.8 ± 2.4	–	–

Hoehn and Yahr values are given as median (range). An average MDS-UPDRS-III score for 19 patients in cohort A was  $38.3 \pm 12.2$  (the score for one PD patient was missing). This score was converted to equivalent UPDRS-III score [39] for a direct comparison with UPDRS motor score of patients in cohort D

UPDRS-III Unified Parkinson's Disease Motor Rating Scale

<sup>a</sup> Age and Disease duration are given as mean ± standard deviation

### Positron emission tomography imaging

All study participants were fasting overnight prior to FDG-PET scanning, but were encouraged to drink plenty of water. Upon acceptance to Department of Nuclear Medicine at University Medical Centre Ljubljana, FDG with activity 250 MBq was intravenously administered to participants using Medrad Intego automatic injector. Participants were placed to rest in a quiet dimly lit room with eyes closed for 30 min. Imaging was performed with low dose attenuation correction CT scan (30 s) followed by 10 min (between 35 and 45 min postinjection) resting state FDG-PET scan of relative glucose metabolism using Siemens Biograph mCT PET/CT scanner. All images were reconstructed into a  $400 \times 400 \times 110$  matrix with a voxel size  $1.02 \times 1.02 \times 3 \text{ mm}^3$  and 4-mm Gaussian postprocessing filter using a Siemens TrueX-TOF iterative algorithm (6 iterations, 21 subsets) which incorporates point-spread-function correction and time-of-flight information.

### Image processing

18F-FDG-PET brain images were converted to Analyze format using MRIConvert software (<http://lcn.uoregon.edu/~jolinda/MRIConvert/>). Then, they were spatially normalized into a standard Montreal Neurological Institute (MNI)-based PET template and smoothed using a Gaussian kernel of  $10 \times 10 \times 10 \text{ mm}$  FWHM, both using SPM5 software (<http://www.fil.ion.ucl.ac.uk/spm/software/SPM5/>), running in Matlab 7.0 (MathWorks Inc., Natick, MA).

### Pattern identification

PDRP-Slovenia principal components were identified from FDG-PET brain images of cohort A by applying an automatic

voxel-based scaled subprofile model/principal component analysis (SSM/PCA; software freely available on <http://www.feinsteinneuroscience.org> at Center for Neuroscience, Feinstein Institute for Medical Research, NY, USA). This operation was performed within a probabilistic gray matter mask created by thresholding and averaging all FDG-PET images in the derivation cohort as described previously [16]. The principal component or a linear combination of several principal components, whose expression in individual images produced the most significant differentiation between PD and NC groups, was determined as a PDRP-Slovenia.

A subject score or PDRP-Slovenia expression in an individual image was Z-transformed using mean and standard deviation of subject scores in the NC group of cohort A, so that the average Z-score of the NC group was set to zero with the standard deviation equal to one.

The reliability of PDRP-Slovenia was estimated using a bootstrapping algorithm [28]. PCA procedure was repeated iteratively for 1000 iterations by resampling the original set of PDRP-Slovenia identification images. For each voxel, the region weight of PDRP-Slovenia was divided by the standard deviation of covariance patterns generated from all iterations which resulted in a map of inverse coefficient of variation (ICV).

### Validation of pattern expression

FDG-PET brain images from cohort B and cohort C were used to validate expression of PDRP-Slovenia in individual subjects for the differentiation between PD, NC, and atypical parkinsonian groups. For this purpose, we used voxel-based TPR algorithm on cohort B and cohort C images to calculate individual scores of PDRP-Slovenia. The resulting scores were then Z-transformed using the mean and standard

deviation value of PDRP-Slovenia NC group described above. We assessed differences in Z-scores between PD and NC groups across cohorts A and B and between PD and NC subjects (cohort B) and atypical parkinsonian groups (cohort C).

### Disease discrimination and clinical correlation

Receiver operating characteristic (ROC) analysis was performed on the newly identified PDRP-Slovenia to evaluate the diagnostic power of its expression for the discrimination of PD patients from normal controls. A cutoff value was determined in cohort A as the point of optimum combination of both high sensitivity and high specificity. The same cutoff value was applied to subject scores in cohort B and cohort C.

We computed correlation coefficients between PDRP-Slovenia subject scores and corresponding clinical ratings for PD subjects in cohort A. Pearson's correlation was used in the case of MDS-UPDRS-III and disease duration whereas non-parametric Spearman's correlation was used in the case of Hoehn and Yahr score.

### Comparison between USA and Slovenia patterns

We quantitatively compared the voxelwise topographies of PDRP-Slovenia and the original PDRP-USA using volume-of-interest (VOI) correlations over the whole brain. VOI comparison was achieved by computing regional weights for a set of 30 standardized VOIs previously defined to encompass key nodes of PD-related subcortical and cortical motor circuitry (see Supplementary file). Voxel-based correlation was also performed between the region weights of spatially equivalent voxels across the two topographic patterns. Moreover, we also compared expression of PDRP-Slovenia and the original PDRP-USA in individual subjects and tested the ability of both networks to differentiate between groups of PD patients and NCs. For this purpose, we used TPR to calculate subject scores of PDRP-USA in PDRP-Slovenia identification subjects (cohort A) and subject scores of PDRP-Slovenia in PDRP-USA identification subjects (cohort D). PDRP-USA subject scores were then compared across PD and NC subjects in cohort A and cohort D. PDRP-Slovenia subject scores were also compared with corresponding PDRP-USA subject scores for PD and NC subjects in cohort A.

Correlations between regional weights of PDRP-Slovenia and PDRP-USA and between their corresponding subject scores in individual subjects were assessed by computing Pearson correlation coefficients. Between-group differences in subject scores were assessed using Student's independent-sample *t* tests.

All statistical analysis was performed using Origin software (OriginLab, Northampton, MA, USA) and considered significant for  $p < 0.05$ . Origin software and Statistical

Parametric Mapping software (Institute of Neurology, UCL, London, UK) were used to create the artwork.

## Results

### PDRP identification

PDRP-Slovenia was identified in cohort A, as the first principal component accounting for 14.5% of subject  $\times$  voxel variance. The pattern (Fig. 1a; Supplementary Fig. S1) was characterized by increased relative metabolic activity in sensorimotor cortex, pallidum, putamen, thalamus, brain stem, and cerebellum associated with decreased relative metabolic activity in posterior parietal, occipital, and frontal cortices. Subject scores of PDRP-Slovenia expression in cohort A were abnormally elevated in PD patients compared to NC subjects ( $p < 0.0001$ ). Bootstrapping algorithm estimated that the topography of PDRP-Slovenia was reliable at  $p < 0.025$  (Supplementary Fig. S2).

### Validation of pattern expression

Subject scores of PDRP-Slovenia expression in cohort B were significantly higher in PD subjects compared to NC subjects ( $p < 0.0001$ ; Fig. 1b). PDRP-Slovenia scores did not differ between cohort A and cohort B for PD subjects ( $p = 0.976$ ) or NC subjects ( $p = 0.062$ ). Subject scores of cohort C patients were significantly different from those of PD subjects ( $p < 0.0001$  for both MSA and PSP), but did not differ from those of NC subjects ( $p = 0.14$  for MSA and  $p = 0.39$  for PSP) in cohort B.

### Disease discrimination and clinical correlation

An optimum cutoff value for diagnosis of PD was a subject score of 1.0, which is associated with sensitivity of 85% and specificity of 90%, determined from the ROC analysis of the identification cohort A data. The sensitivity and specificity of 84 and 90% were found by applying the same cutoff value to cohort B subject scores. This analysis confirmed that PDRP-Slovenia expression significantly discriminates PD and NC subjects in cohorts A and B (both at  $p < 0.001$ ).

Subject scores of PDRP-Slovenia expression in PD subjects from cohort A correlated positively with MDS-UPDRS-III scores and Hoehn and Yahr score as presented in Fig. 2, but not with disease duration.

### Comparison between USA and Slovenia patterns

Comparison between spatial topographies of the original PDRP-USA and PDRP-Slovenia showed significant correlations in region weights (Fig. 3a; for data, see Supplementary

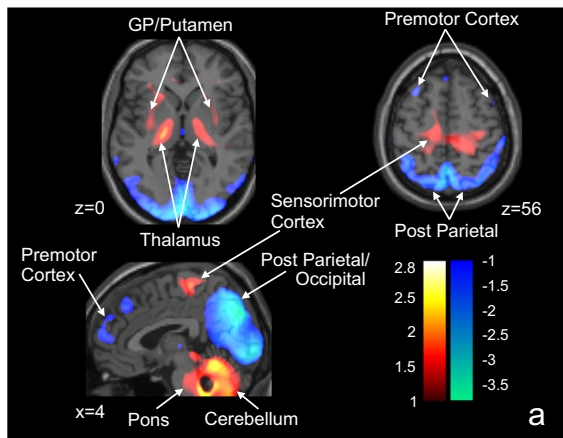
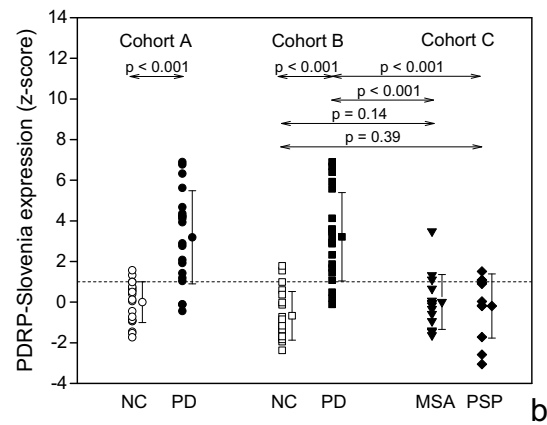


**Fig. 1 a** PDRP-Slovenia: Parkinson’s disease-related pattern identified by network analysis of FDG-PET scans from 20 PD patients and 20 age-matched normal controls in cohort A. Relative metabolic increases are represented by voxels with positive region weights and are color-coded red to yellow (sensorimotor cortex, pallidum, putamen, thalamus, brain stem, and cerebellum), whereas associated metabolic decreases are represented by voxels with negative region weights and are color-coded blue to purple (posterior parietal, occipital, and frontal cortices). **b** Subject scores of PDRP-Slovenia for the PD and NC subjects of pattern



identification (cohort A), for the PD and NC subjects of pattern validation (cohort B), and for patients with MSA and PSP (cohort C). Pattern expression significantly differentiated PD from NC subjects in cohorts A and B and cohort C patients with atypical parkinsonism from PD patients but did not differ significantly between the two PD groups or the two NC groups and between the atypical parkinsonian patients and both NC groups. Group mean values and standard deviations are plotted besides group individual values. Horizontal dashed line marks the optimal cutoff value based on ROC analysis in pattern identification cohort A

file) using both the standardized set of VOIs ( $r = 0.860$ ,  $p < 0.001$ ) as well as the voxel-based analysis ( $r = 0.945$ ,  $p < 0.001$ ).

Subject scores of the original PDRP-USA expression were found to be significantly elevated in PD subjects compared to NCs in cohort A ( $p < 0.001$ ) and in cohort D ( $p < 0.001$ ; Fig. 3b), but were not significantly different between NC subjects in cohorts A and D ( $p = 0.438$ ). The difference in PDRP-USA expression between PD subjects in cohorts A and D was on the borderline of significance ( $p = 0.051$ ). We confirmed a high correlation between subject scores of PDRP-USA and PDRP-Slovenia expression for the combined group of PD and NC subjects ( $r = 0.977$ ,  $p < 0.001$ ; Fig. 3c) from cohort A. High correlation was also observed for separate PD ( $r = 0.967$ ,  $p < 0.001$ ) and NC groups ( $r = 0.946$ ,  $p < 0.001$ ).

**Discussion**

In this study, we reproduced PDRP in a Slovenian cohort of clinically diagnosed PD patients using FDG-PET brain images and SSM/PCA network analysis; we call it PDRP-Slovenia. Expression of PDRP-Slovenia was significantly elevated in PD patients compared to healthy controls in both identification and validation cohorts but was not elevated in patients with atypical parkinsonism. We decided to scan the PD patients in validation cohort B on dopaminergic treatment because it is a burden for them to stay without treatment for many hours. It has been shown in a previous study [24] that levodopa treatment reduces the expression of PDRP. Therefore, dopaminergic treatment, if anything, decreased the PDRP expression in our validation PD group and made the differentiation between patients

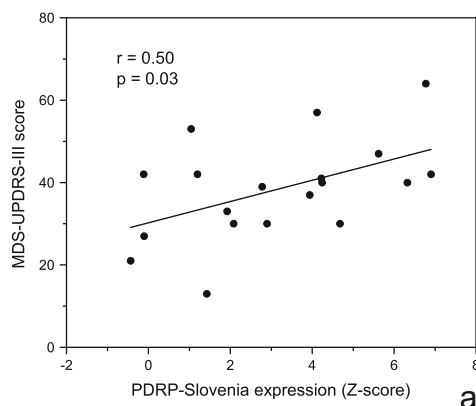
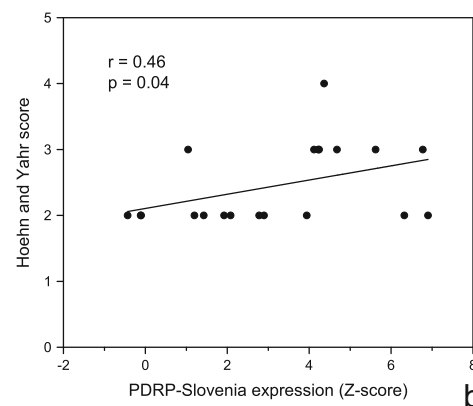


**Fig. 2** Correlations between subject scores of PDRP-Slovenia expression and corresponding clinical ratings for PD patients in identification cohort A. Significant correlation with PDRP-Slovenia expression was found for **a** MDS-UPDRS-III score ( $N = 19$ ; Pearson’s correlation) and



**b** Hoehn and Yahr score ( $N = 20$ ; non-parametric Spearman’s correlation). MDS-UPDRS-III average score was calculated for 19 patients since the score for one PD patient was missing

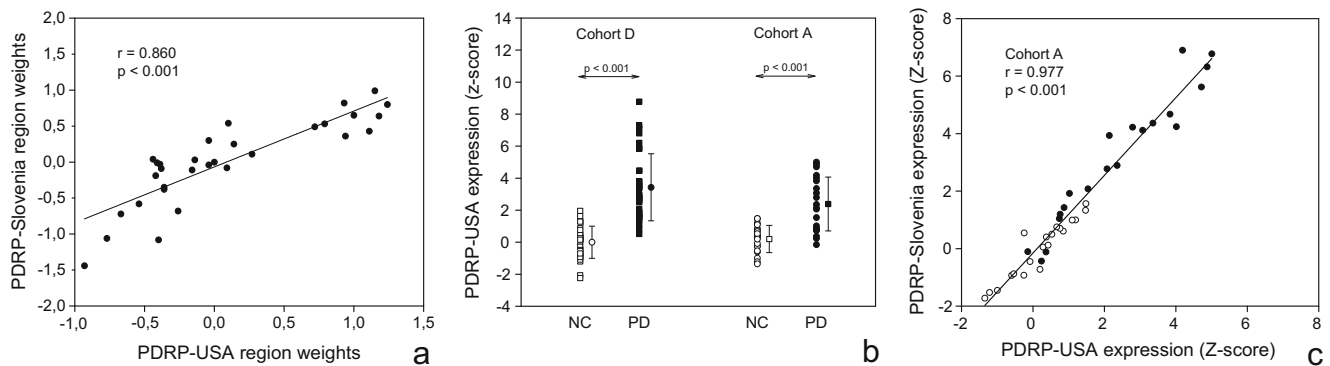


**Fig. 3** Comparison between PDRP-Slovenia and original PDRP-USA identified at the Feinstein Institute for Medical Research in NY, USA. **a** Regional weights in the standardized set of VOIs covering whole brain correlated significantly for the two patterns. **b** Subject scores of PDRP-USA expression for the PDRP-USA identification PD and NC subjects (cohort D) and for PDRP-Slovenia identification PD and NC subjects

(cohort A); pattern expression significantly differentiated PD and NC subjects in both cohorts; group mean values and standard deviations are plotted besides group individual values. **c** Subject scores of PDRP-USA expression in PD (*filled circles*) and NC subjects (*open circles*) from cohort A highly correlated with corresponding subject scores of PDRP-Slovenia expression

and controls even less pronounced. Although the normal healthy subjects in cohort B were 8 years younger than PD patients, we believe that this age difference did not play any important role in the validation of PDRP. It has been shown in previous studies that the normal aging process does not affect the expression of PDRP [25, 26]. The metabolic topography of normal aging has been identified previously too, and it is topographically different from PDRP [27].

Very good diagnostic accuracy for distinguishing between PD patients and healthy controls was demonstrated by ROC analysis with specificity and sensitivity of 85–90% for both identification and validation cohorts at the optimal pattern expression cutoff. This level of discrimination power is in the range of previously reported values for the American, Chinese, and Dutch cohorts [19, 20, 28]. In addition, we confirmed that PDRP is specific from the preliminary results showing that PDRP-Slovenia could distinguish PD from atypical parkinsonism (Fig. 1b). PDRP has also been shown to be able to differentiate PD from MSA patients scanned with perfusion single-photon emission computed tomography (SPECT) [29], as well as to detect the early metabolic brain changes in prodromal disease phases [30, 31]. To further validate a Slovenian PDRP, a prospective study is underway in patients with shorter disease duration who will be followed prospectively, as well as in a larger group of patients with atypical parkinsonism. Additionally, a prospective study would also be warranted to evaluate the ability of widely available dopamine transporter SPECT and 131I/123I-Metaiodobenzylguanidine (mIBG) heart scintigraphy to differentiate between PD and atypical parkinsonism in comparison to PDRP analysis.

In this study, we confirmed the similarity between the newly identified PDRP-Slovenia and the original American PDRP [11] by showing that the region weights describing spatial topography highly correlate between the two patterns and the corresponding subject scores of both patterns also strongly correlate for PD and NC subjects. Both patterns were also

topographically comparable to those generated in China, Dutch, and India cohorts as briefly noted in a study on the similarity of brain networks [32]. Of note, all PDRPs were generally similar to the homologous parkinsonism-related pattern (PRP) produced with FDG-PET in MPTP-lesioned parkinsonian macaques [33, 34]. Analogous to the properties of PDRP in patients, the expression of PRP correlated with motor ratings and was modulated by experimental therapeutics with striatal cell implantation in parkinsonian macaques. These patterns identified with multivariate SSM analysis are all consistent with characteristic distributions of abnormal relative brain metabolism detected using high-resolution FDG-PET imaging with univariate SPM analysis in early stage PD patients [6, 35, 36] and in parkinsonian macaques [34]. Moreover, increased glucose metabolism in the corresponding subcortical regions was also reported by quantitative [ $^{11}\text{C}$ ]-2-deoxy- glucose autoradiography in various experimental animal models of PD [37–39].

These findings clearly confirm the robustness of PDRP despite the fact that subjects in Slovenian cohorts, and all other cohorts were scanned with different equipment and scanning protocols. It also shows that Z-transformation using mean and standard deviation value of the NC group in the identification cohort resulted in highly comparable subject scores in absolute terms.

We also confirmed the findings in the previous publications of positive correlations between PDRP-Slovenia expression and corresponding individual values of MDS-UPDRS-III and Hoehn and Yahr score [18, 19] at statistically significant levels. Correlation of the PDRP-Slovenia expression with clinical ratings suggests that the regional metabolic dysfunction contained in PDRP-Slovenia brain topography is closely linked to PD motor symptoms.

It is worth noting that motor symptoms of PD patients in cohort A and cohort D were assessed using MDS-UPDRS-III and UPDRS-III, respectively. MDS-UPDRS tends to give rise

to higher motor scores due to the inclusion of additional items in the revised UPDRS. To reconcile apparent differences in motor scores between the Slovenian and American patients in our study, we converted individual scores of the patients in cohort A from MDS-UPDRS-III to UPDRS-III using published conversion formulas [40]. The motor scores in UPDRS-III were slightly lower in cohort A patients (see Table 1) than in cohort D patients but had no significant differences between these two groups. This could partially explain the borderline reduction in PDRP scores in the patients in cohort A compared to those in cohort D (Fig. 3b) indicating less severity of the disease and less dopaminergic deficit in the Slovenian patients given that striatal dopaminergic dysfunction correlated negatively with both UPDRS motor ratings and PDRP scores in the same patient cohort over the course of disease progression [7].

Within PDRP-Slovenia, we observe relatively increased metabolic activity in sensorimotor cortex, pallidum, putamen, thalamic, brain stem, and cerebellum, along with relatively decreased metabolic activity in posterior parietal/occipital regions and to a lesser extent in the frontal cortex, consistent with the originally identified pattern [11]. In line with previous publications, the PDRP-Slovenia involves metabolic changes at key nodes of the cortico-striatopallido-thalamo-cortical (CSPTC) circuits and related cerebello-cortical pathways [16, 18, 19], which are generally associated with pathophysiology of PD and primarily characterized by enhanced pallido-thalamic inhibition [41]. Although the positive regions of the PDRP topography and the reliability map are located primarily in gray matter, some of them such as cerebellum and motor cortex also extend to some degree into white matter (Fig. 1a; Supplementary Figs. S1 and S2). This is caused by the use of the probabilistic gray matter mask in network analysis which could include very small portion of white matter, and inevitably, the limited resolution of reconstructed FDG-PET images. It would be of interest to further investigate relative contributions of different brain tissue types to PDRP topography both inside and outside the gray matter space defined by FDG-PET or MRI brain images.

It has to be emphasized that spatial covariance patterns describe functional connectivity of spatially distributed brain regions of relatively increased and decreased metabolic activity and serve as an excellent representation of neurodegenerative processes that may not be fully accounted for by evaluation of local metabolic values or by voxel-based comparison of FDG-PET images between subject groups based on univariate SPM analysis. In addition to PET and SPECT imaging, multivariate SSM analysis has also been proven successful with MRI in PD and other neurodegenerative diseases. For example, PDRP expression measured prospectively using cerebral blood flow from arterial spin labeling (ASL) perfusion MRI was comparable to that obtained from FDG-PET images in PD patients [26]. ASL MRI and SSM analysis were further

used for the identification of PDRP [42] and an Alzheimer's disease-related covariance pattern [43]. Recently, a PD-related network has been found using resting-state functional MRI [44] as well. Anatomical MRI data was used to generate structural covariance patterns associated with normal aging in humans [45, 46] and in rhesus macaques [47]. Hence, SSM/PCA is a generic methodology for generation of specific brain networks using different functional and structural imaging modalities.

The parietal and occipital regions with relatively decreased metabolic activity observed in PDRP-Slovenia, as well as less pronounced relatively decreased frontal metabolic activity compared to the original PDRP, may be related to differences in non-motor symptoms in PD cohorts [19]. It has been suggested that relatively decreased metabolic activity findings in PD might not be associated only with motor control systems [19, 48, 49] but also with cognitive deficits even in patients without apparent cognitive impairment [48]. Less pronounced decreases in relative metabolism of frontal regions in PDRP-Slovenia is not entirely understood. It may, however, reflect less dopaminergic deficit in Slovenian identification patient group compared to the original American one discussed above. The pathological substrate of the cognitive impairment in PD is heterogeneous, involving different pathological and neurotransmitter changes [49, 50]. Dopamine deficiency in frontostriatal pathways reflects in some way relatively decreased metabolic activity in frontal regions, whereas relatively decreased metabolic activity in parietal regions is related to cholinergic cortical deficits [51]. These interesting observations of minor deviations in PDRP regional topography are worth further exploration in relation to PD subjects' demographic, clinical, and behavioral data, and might offer greater insight into pathophysiology underlying PD symptoms.

## Conclusion

In summary, we have applied SSM/PCA analysis to identify PD-related brain network pattern in a cohort of 20 PD patients and 20 controls, PDRP-Slovenia, which significantly discriminates two groups of PD patients from healthy controls and from atypical parkinsonian groups and reproduces anatomical brain networks and specific metabolic changes associated with clinical manifestations of PD. PDRP-Slovenia was also validated by showing that (i) its expression correlates with clinical motor scores of PD patients; (ii) its expression yields a good diagnostic accuracy; and (iii) its topography and expression agree very well with the original PDRP. Our results confirmed the findings of the previous studies and further proved that PDRP network provides a reproducible objective imaging biomarker of clinical disability in PD independent of patient population, PET scanners, and imaging protocols. PDRP calculation can be easily incorporated into FDG-PET

brain imaging routine to assess network expression in single cases for disease discrimination or clinical correlations and to track inherent functional changes in PD associated with disease progression and therapeutic outcome.

#### Compliance with ethical standards

**Funding** This work was supported by the Slovenian Research Agency (L3-4255). The work of YM, SP, VD and DE was supported by the NIH Morris K Udall Center of Excellence for Parkinson's Disease Research (P50 NS071675).

**Conflict of interest** The authors declare that they have no conflict of interest.

**Ethical approval** All procedures performed in the studies involving human participants were in accordance with the ethical standards of the Slovenian Medical Ethics Committee and with the 1964 Helsinki Declaration and its later amendments or comparable ethical standards.

**Informed consent** Informed consent was obtained from all individual participants included in the study.

#### References

- Hughes AJ, Daniel SE, Kilford L, Lees AJ (1992) Accuracy of clinical diagnosis of idiopathic Parkinson's disease: a clinicopathological study of 100 cases. *J Neurol Neurosurg Psychiatry* 55:181–184. doi:10.1136/jnnp.55.3.181
- Joutsa J, Gardberg M, R oytt  M, Kaasinen V (2014) Diagnostic accuracy of parkinsonism syndromes by general neurologists. *Park Relat Disord* 20:840–844. doi:10.1016/j.parkreldis.2014.04.019
- Juh R, Kim J, Moon D, Choe B, Suh T (2004) Different metabolic patterns analysis of parkinsonism on the 18F-FDG PET. *Eur J Radiol* 51:223–233. doi:10.1016/S0720-048X(03)00214-6
- Tang CC, Eidelberg D (2010) Abnormal metabolic brain networks in Parkinson's disease: from blackboard to bedside. *Prog Brain Res* 184:161–176. doi:10.1016/S0079-6123(10)84008-7
- Tatsch K (2010) Positron emission tomography in diagnosis and differential diagnosis of Parkinson's disease. *Neurodegener Dis* 7:330–340. doi:10.1159/000314499
- Teune LK, Bartels AL, De Jong BM, Willemsen ATM, Eshuis SA, De Vries JJ, Van Oostrom JCH, Leenders KL (2010) Typical cerebral metabolic patterns in neurodegenerative brain diseases. *Mov Disord* 25:2395–2404. doi:10.1002/mds.23291
- Huang C, Tang C, Feigin A, Lesser M, Ma Y, Pourfar M, Dhawan V, Eidelberg D (2007) Changes in network activity with the progression of Parkinson's disease. *Brain* 130:1834–1846. doi:10.1093/brain/awm086
- Politis M (2014) Neuroimaging in Parkinson disease: from research setting to clinical practice. *Nat Rev Neurol* 10:708–722. doi:10.1038/nrneurol.2014.205
- Postuma RB, Berg D, Stern M, Poewe W, Olanow CW, Oertel W, Obeso J, Marek K, Litvan I, Lang AE, Halliday G, Goetz CG, Gasser T, Dubois B, Chan P, Bloem BR, Adler CH, Deuschl G (2015) MDS clinical diagnostic criteria for Parkinson's disease. *Mov Disord* 30:1591–1601. doi:10.1002/mds.26424
- Moeller JR, Strother SC (1991) A regional covariance approach to the analysis of functional patterns in positron emission tomographic data. *J Cereb Blood Flow Metab* 11:A121–A135. doi:10.1038/jcbfm.1991.47
- Ma Y, Tang C, Spetsieris PG, Dhawan V, Eidelberg D (2007) Abnormal metabolic network activity in Parkinson's disease: test-retest reproducibility. *J Cereb Blood Flow Metab* 27:597–605
- Eckert T, Tang C, Ma Y, Brown N, Lin T, Frucht S, Feigin A, Eidelberg D (2008) Abnormal metabolic networks in atypical parkinsonism. *Mov Disord* 23:727–733. doi:10.1002/mds.21933
- Poston KL, Tang CC, Eckert T, Dhawan V, Frucht S, Vonsattel JP, Fahn S, Eidelberg D (2012) Network correlates of disease severity in multiple system atrophy. *Neurology* 78:1237–1244. doi:10.1212/WNL.0b013e318250d7fd
- Niethammer M, Tang CC, Feigin A, Allen PJ, Heinen L, Hellwig S, Amtage F, Hanspal E, Vonsattel JP, Poston KL, Meyer PT, Leenders KL, Eidelberg D (2014) A disease-specific metabolic brain network associated with corticobasal degeneration. *Brain* 137:3036–3046. doi:10.1093/brain/awu256
- Spetsieris PG, Eidelberg D (2011) Scaled subprofile modeling of resting state imaging data in Parkinson's disease: methodological issues. *NeuroImage* 54:2899–2914. doi:10.1016/j.neuroimage.2010.10.025
- Tang CC, Poston KL, Eckert T, Feigin A, Frucht S, Gudesblatt M, Dhawan V, Lesser M, Vonsattel J-P, Fahn S, Eidelberg D (2010) Differential diagnosis of parkinsonism: a metabolic imaging study using pattern analysis. *Lancet Neurol* 9:149–158. doi:10.1016/S1474-4422(10)70002-8
- Tripathi M, Tang CC, Feigin A, De Lucia I, Nazem A, Dhawan V, Eidelberg D (2016) Automated differential diagnosis of early parkinsonism using metabolic brain networks: a validation study. *J Nucl Med* 57:60–66. doi:10.2967/jnumed.115.161992
- Eidelberg D (2009) Metabolic brain networks in neurodegenerative disorders: a functional imaging approach. *Trends Neurosci* 32:548–557. doi:10.1016/j.tins.2009.06.003
- Wu P, Wang J, Peng S, Ma Y, Zhang H, Guan Y, Zuo C (2013) Metabolic brain network in the Chinese patients with Parkinson's disease based on 18F-FDG PET imaging. *Parkinsonism Relat Disord* 19:622–627. doi:10.1016/j.parkreldis.2013.02.013
- Teune LK, Renken RJ, Mudali D, De Jong BM, Dierckx RA, Roerdink JBTM, Leenders KL (2013) Validation of parkinsonian disease-related metabolic brain patterns. *Mov Disord* 28:547–551. doi:10.1002/mds.25361
- Holtbernd F, Ma Y, Peng S, Schwartz F, Timmermann L, Kracht L, Fink GR, Tang CC, Eidelberg D, Eggers C (2015) Dopaminergic correlates of metabolic network activity in Parkinson's disease. *Hum Brain Mapp* 36:3575–3585. doi:10.1002/hbm.22863
- Poston KL, Eidelberg D (2009) Network biomarkers for the diagnosis and treatment of movement disorders. *Neurobiol Dis* 35:141–147. doi:10.1016/j.nbd.2008.09.026
- Gibb WR, Lees AJ (1988) Occasional review: the relevance of the Lewy body to the pathogenesis of idiopathic Parkinson's disease. *J Neurol Neurosurg Psychiatry* 51:745–752. doi:10.1136/jnnp.51.6.745
- Feigin A, Fukuda M, Dhawan V, Przedborski S, Jackson-Lewis V, Mentis MJ, Moeller JR, Eidelberg D (2001) Metabolic correlates of levodopa response in Parkinson's disease. *Neurology* 57:2083–2088. doi:10.1212/WNL.57.11.2083
- Moeller JR, Nakamura T, Mentis MJ, Dhawan V, Spetsieris P, Antonini A, Missimer J, Leenders KL, Eidelberg D (1999) Reproducibility of regional metabolic covariance patterns: comparison of four populations. *J Nucl Med* 40:1264–1269. doi:10.1016/B978-012161340-2/50039-1
- Ma Y, Huang C, Dyke JP, Pan H, Alsop D, Feigin A, Eidelberg D (2010) Parkinson's disease spatial covariance pattern: noninvasive quantification with perfusion MRI. *J Cereb Blood Flow Metab* 30:505–509. doi:10.1038/jcbfm.2009.256
- Moeller JR, Ishikawa T, Dhawan V, Spetsieris P, Mandel F, Alexander GE, Grady C, Pietrini P, Eidelberg D (1996) The



- metabolic topography of normal aging. *J Cereb Blood Flow Metab* 16:385–398. doi:10.1097/00004647-199605000-00005
28. Peng S, Ma Y, Spetsieris PG, Mattis P, Feigin A, Dhawan V, Eidelberg D (2014) Characterization of disease-related covariance topographies with SSMPCA toolbox: effects of spatial normalization and PET scanners. *Hum Brain Mapp* 35:1801–1814. doi:10.1002/hbm.22295
  29. Eckert T, Van Laere K, Tang C, Lewis DE, Edwards C, Santens P, Eidelberg D (2007) Quantification of Parkinson's disease-related network expression with ECD SPECT. *Eur J Nucl Med Mol Imaging* 34:496–501. doi:10.1007/s00259-006-0261-9
  30. Holtbernd F, Gagnon J-F, Postuma RB, Ma Y, Tang CC, Feigin A, Dhawan V, Vendette M, Soucy J-P, Eidelberg D, Montplaisir J (2014) Abnormal metabolic network activity in REM sleep behavior disorder. *Neurology* 82:620–627. doi:10.1212/WNL.0000000000000130
  31. Wu P, Yu H, Peng S, Dauvilliers Y, Wang J, Ge J, Zhang H, Eidelberg D, Ma Y, Zuo C (2014) Consistent abnormalities in metabolic network activity in idiopathic rapid eye movement sleep behaviour disorder. *Brain* 137:3122–3128. doi:10.1093/brain/awu290
  32. Ko JH, Spetsieris P, Ma Y, Dhawan V, Eidelberg D (2014) Quantifying significance of topographical similarities of disease-related brain metabolic patterns. *PLoS One* 9:e88119. doi:10.1371/journal.pone.0088119
  33. Ma Y, Peng S, Spetsieris PG, Sossi V, Eidelberg D, Doudet DJ (2012) Abnormal metabolic brain networks in a nonhuman primate model of parkinsonism. *J Cereb Blood Flow Metab* 32:633–642. doi:10.1038/jcbfm.2011.166
  34. Peng S, Ma Y, Flores J, Cornfeldt M, Mitrovic B, Eidelberg D, Doudet DJ (2016) Modulation of abnormal metabolic brain networks by experimental therapies in a nonhuman primate model of Parkinson's disease: an application to human retinal pigment epithelial (hRPE) cell implantation. *J Nucl Med* 57:1591–1598
  35. Borghammer P, Hansen SB, Eggers C, Chakravarty M, Vang K, Aanerud J, Hilker R, Heiss WD, Rodell A, Munk OL, Keator D, Gjedde A (2012) Glucose metabolism in small subcortical structures in Parkinson's disease. *Acta Neurol Scand* 125:303–310. doi:10.1111/j.1600-0404.2011.01556.x
  36. Eggers C, Hilker R, Burghaus L, Schumacher B, Heiss WD (2009) High resolution positron emission tomography demonstrates basal ganglia dysfunction in early Parkinson's disease. *J Neurol Sci* 276:27–30. doi:10.1016/j.jns.2008.08.029
  37. Mitchell IJ, Clarke CE, Boyce S, Robertson RG, Peggs D, Sambrook MA, Crossman AR (1989) Neural mechanisms underlying parkinsonian symptoms based upon regional uptake of 2-deoxyglucose in monkeys exposed to 1-methyl-4-phenyl-1,2,3,6-tetrahydropyridine. *Neuroscience* 32:213–226
  38. Guigoni C, Li Q, Aubert I, Dovero S, Bioulac BH, Bloch B, Crossman AR, Gross CE, Bezard E (2005) Involvement of sensorimotor, limbic, and associative basal ganglia domains in L-3,4-dihydroxyphenylalanine-induced dyskinesia. *J Neurosci* 25:2102–2107
  39. Carlson JD, Pearlstein RD, Buchholz J, Iacono RP, Maeda G (1999) Regional metabolic changes in the pedunclopontine nucleus of unilateral 6-hydroxydopamine Parkinson's model rats. *Brain Res* 828:12–19
  40. Goetz CG, Stebbins GT, Tilley BC (2012) Calibration of unified Parkinson's disease rating scale scores to Movement Disorder Society-unified Parkinson's disease rating scale scores. *Mov Disord* 27:1239–1242. doi:10.1002/mds.25122
  41. Wichmann T, DeLong MR (2007) Anatomy and physiology of the basal ganglia: relevance to Parkinson's disease and related disorders. *Handb Clin Neurol* 83:1–18. doi:10.1016/S0072-9752(07)83001-6
  42. Melzer TR, Watts R, MacAskill MR, Pearson JF, Rueger S, Pitcher TL, Livingston L, Graham C, Keenan R, Shankaranarayanan A, Alsop DC, Dalrymple-Alford JC, Anderson TJ (2011) Arterial spin labelling reveals an abnormal cerebral perfusion pattern in Parkinson's disease. *Brain* 134:845–855. doi:10.1093/brain/awq377
  43. Asllani I, Habeck C, Scarmeas N, Borogovac A, Brown TR, Stern Y (2008) Multivariate and univariate analysis of continuous arterial spin labeling perfusion MRI in Alzheimer's disease. *J Cereb Blood Flow Metab* 28:725–736. doi:10.1038/sj.jcbfm.9600570
  44. Wu T, Ma Y, Zheng Z, Peng S, Wu X, Eidelberg D, Chan P (2015) Parkinson's disease-related spatial covariance pattern identified with resting-state functional MRI. *J Cereb Blood Flow Metab* 35:1764–1770. doi:10.1038/jcbfm.2015.118
  45. Bergfield KL, Hanson KD, Chen K, Teipel SJ, Hampel H, Rapoport SI, Moeller JR, Alexander GE (2010) Age-related networks of regional covariance in MRI gray matter: reproducible multivariate patterns in healthy aging. *NeuroImage* 49:1750–1759. doi:10.1016/j.neuroimage.2009.09.051
  46. Brickman AM, Habeck C, Ramos MA, Scarmeas N, Stern Y (2008) A forward application of age associated gray and white matter networks. *Hum Brain Mapp* 29:1139–1146. doi:10.1002/hbm.20452
  47. Alexander GE, Chen K, Aschenbrenner M, Merkley TL, Santerre-Lemmon LE, Shamy JL, Skaggs WE, Buonocore MH, Rapp PR, Barnes CA (2008) Age-related regional network of magnetic resonance imaging gray matter in the rhesus macaque. *J Neurosci* 28:2710–2718. doi:10.1523/JNEUROSCI.1852-07.2008
  48. M. Niethammer, A. Feigin, D. Eidelberg (2012) Functional neuroimaging in Parkinson's disease. *Cold Spring Harb Perspect Med* 2 doi:10.1101/cshperspect.a009274
  49. Dickson DW, Fujishiro H, Orr C, DelleDonne A, Josephs KA, Frigerio R, Burnett M, Parisi JE, Klos KJ, Ahlskog JE (2009) Neuropathology of non-motor features of Parkinson disease. *Park Relat Disord* 15:S1–S5. doi:10.1016/S1353-8020(09)70769-2
  50. Pletnikova O, West N, Lee MK, Rudow GL, Skolasky RL, Dawson TM, Marsh L, Troncoso JC (2005) Abeta deposition is associated with enhanced cortical alpha-synuclein lesions in Lewy body diseases. *Neurobiol Aging* 26:1183–1192. doi:10.1016/j.neurobiolaging.2004.10.006
  51. Hilker R, Thomas AV, Klein JC, Weisenbach S, Kalbe E, Burghaus L, Jacobs AH, Herholz K, Heiss WD (2005) Dementia in Parkinson disease: functional imaging of cholinergic and dopaminergic pathways. *Neurology* 65:1716–1722. doi:10.1212/01.wnl.0000191154.78131.f6